

Microscopic origin of polarity in quasiamorphous BaTiO₃A. I. Frenkel,¹ Y. Feldman,² V. Lyahovitskaya,² E. Wachtel,² and I. Lubomirsky²¹*Physics Department, Yeshiva University, 245 Lexington Avenue, New York, New York 10016, USA*²*Weizmann Institute of Science, Rehovot 76100, Israel*

(Received 10 September 2004; published 28 January 2005; corrected 8 February 2005)

The recent observation of pyroelectricity in quasiamorphous thin films of BaTiO₃ introduced a previously unreported type of polar ionic solid where the appearance of a macroscopic dipole moment is not accompanied by long-range crystal-like order. This poses a question regarding the mechanism of polarity in noncrystalline ionic systems and the nature of their local dipoles. By combining x-ray diffraction and x-ray-absorption fine-structure spectroscopy techniques we have identified the local dipoles as stable but distorted TiO₆ octahedra. The magnitude of the off-center displacement of the Ti ion and the concomitant dipole moment in both quasiamorphous (polar) and amorphous (nonpolar) BaTiO₃ were found to be nearly twice as large as those in bulk BaTiO₃. We propose that the mechanism of macroscopic polarity in quasiamorphous BaTiO₃ is in a weak orientational ordering of the TiO₆ bonding units. In this view, one may expect that other amorphous ionic oxides containing stable local bonding units, for example NbO₆, TiO₆, or VO₆, may also form noncrystalline polar phases.

DOI: 10.1103/PhysRevB.71.024116

PACS number(s): 61.10.Ht, 61.43.Er, 64.70.Nd

It has been reported recently¹ that amorphous BaTiO₃ thin films on Si (100) prepared by radio frequency (RF) magnetron sputtering do not crystallize if pulled through a temperature gradient. According to x-ray and electron diffraction these films remain noncrystalline below 700 °C, which is the temperature that normally leads to rapid crystallization of BaTiO₃. These films nevertheless exhibit significant (5–15 % of bulk BaTiO₃) pyroelectric and piezoelectric effects, indicating that the phase is polar. This noncrystalline but polar phase was named quasiamorphous, in contrast to the as-deposited amorphous phase that is neither pyroelectric nor piezoelectric and therefore nonpolar.^{1,2} This paper investigates the nature of this surprising effect in disordered films.

The origin of polarity in ionic solids is generally associated with crystallinity.^{3,4} Nevertheless, quasiamorphous films with no crystallites at all are pyroelectric, whereas partially crystallized films (amorphous matrix containing nanocrystallites) are not. This agrees with the fact that nanocrystalline BaTiO₃ with grains smaller than ≈30 nm is usually not ferroelectric^{5–10} with the exception of some special cases.^{11,12} This also implies that the quasiamorphous phase is not a transient state between the amorphous and the crystalline phases and that the origin of polarity in quasiamorphous films remains to be determined. Polarity in quasiamorphous films is particularly surprising because amorphous BaTiO₃ is not expected to form a stable network of covalent bonds (it is >85% ionic¹³) and must be viewed as a dense random packing of hard spheres,² which is kinetically stabilized. It is thus expected to be neither polar nor thermally stable. It has been suggested that the steep temperature gradient employed during formation of the quasiamorphous films generates a gradient of mechanical strain. The latter causes orientational ordering of hypothetical crystal motifs (the regions with short-range order on the scale of one or two unit cells, i.e., below the detection limit by TEM) and, consequently, the macroscopic polarity of the quasiamorphous phase.¹ However, the nature of these hypothetical crystal motifs that ef-

fectively function as dipoles, as well as the degree of their ordering remain uncertain.

Elucidating the microscopic origin of polarity in quasiamorphous BaTiO₃ requires direct measurement of the local bonding geometry of the Ti atom. Therefore x-ray-absorption fine-structure (XAFS) spectroscopy was chosen as the most appropriate technique for this purpose. The XAFS technique is sensitive to short-range order only and is thus particularly valuable for structural determination when long-range periodicity is absent. For BaTiO₃, XAFS measurements directly confirmed previous experimental^{14,15} and theoretical¹⁶ results that Ti atoms are displaced in the [111] direction of the TiO₆ octahedral bonding units within a very wide range of temperatures¹⁷ and grain sizes.¹⁸ Similar behavior of the Nb [111] displacement in KNbO₃ was demonstrated by XAFS as a function of pressure.¹⁹

For the current studies, 100–180-nm-thick quasiamorphous BaTiO₃ films were prepared by pulling as-deposited amorphous RF sputtered films through a temperature gradient with peak temperature of 600 °C. A compressive stress of $\sigma=2.0\text{--}2.2$ GPa developed in the films which were passed through the temperature gradient. The details of the experimental procedure are given in Ref. 1. For comparison, three other types of samples were measured as well: as-deposited amorphous films; polycrystalline films prepared by annealing as-deposited films under isothermal conditions at 600 °C; and partially crystallized films (amorphous matrix with clearly detectable nanocrystallites). The presence of the nanocrystallites in the partially crystallized samples was detected by electron diffraction performed in the transmission electron microscope (TEM Phillips CM-120). No indication of crystallites as small as three to five unit cells was found in the quasiamorphous films either by electron diffraction [Fig. 1(a)] or by using different x-ray-diffraction (XRD) scanning protocols including 2θ scans at fixed θ , and pole figure measurements. The XRD patterns (θ - 2θ scans, Rigaku D-Max/B diffractometer) of the quasiamorphous films and the as-deposited films were indistinguishable [Fig. 1(b)]. Scanning

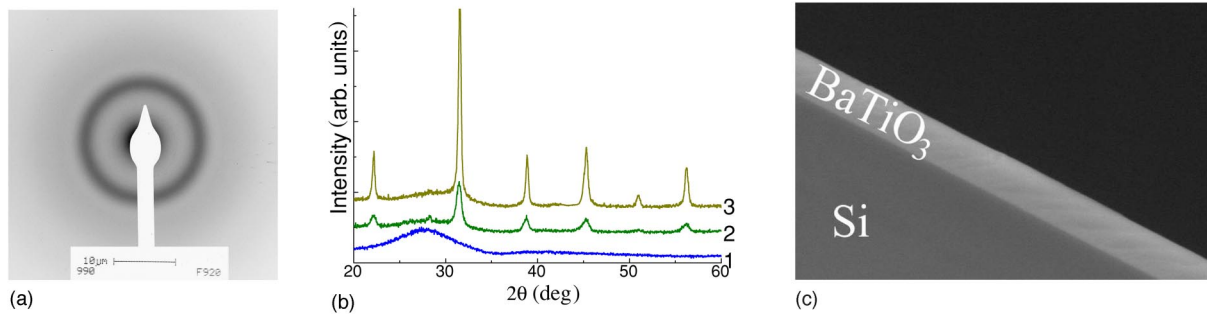


FIG. 1. (Color online) (a) Electron-diffraction pattern of quasiamorphous BaTiO₃; (b) XRD patterns (θ - 2θ scans) of BaTiO₃ films: (i) quasiamorphous, S4 (identical to the as-deposited amorphous); (ii) partially crystallized sample containing nanocrystallites, S6; (iii) polycrystalline sample, S8. (c) SEM image (secondary electron mode, cross section) of a 180-nm-thick quasiamorphous BaTiO₃ film.

electron microscopy images of the amorphous and quasiamorphous films appeared to be identical and did not reveal voids and/or cracks [Fig. 1(c)]. The patterns of both the polycrystalline and the partially crystallized films were consistent with those of cubic (or tetragonal) BaTiO₃. The intensities of the diffraction peaks for the partially crystallized samples were significantly lower (Fig. 1) because part of the film remained in the amorphous phase. The discrimination between cubic and tetragonal phases of BaTiO₃ was not possible due to grain-size related broadening of the peaks.

Ti *K*-edge x-ray-absorption spectra of the BaTiO₃ thin films and of the coarse powder reference samples of BaTiO₃ and EuTiO₃, with grain size of 1–10 μm , were measured at the National Synchrotron Light Source (NSLS), beam line X16C, at Brookhaven National Laboratory. The experimental details were similar to those used previously for the investigation of BaTiO₃.¹⁸

According to the x-ray-absorption near-edge structure (XANES) data, two groups of samples can be distinguished, in excellent agreement with XRD data: (i) the crystalline-like, S6-S8 [Fig. 2(a)], the amorphous-like, S1-S5 [Fig. 2(b)]. For all the samples from the crystalline-like group, peak A (4967 eV), shoulder B (4979 eV), and the $1s$ - $4p$ resonance C (4984 eV) are well pronounced [Fig. 2(a)]. For the group S1-S5 only the peak A is pronounced [Fig. 2(b)]. XANES spectral features for different titanium oxide compounds were investigated both experimentally and theoretically, by Farges *et al.*^{20–24} and Wu.²⁵ The feature A [Figs. 2(a)–2(c) insets] is located in the region corresponding to the $1s$ - $3d$ transition. This transition is dipole forbidden in the atom by the $\Delta L=1$ selection rule.²⁶ In order to contribute significantly to XANES in this range of energies, the final state of the photoelectron must have some p -like character in the solid, via hybridization between Ti $3d$ and O $2p$ orbitals.²⁷ This may occur only if the Ti atom is displaced away from the center of inversion symmetry (e.g., off center of the Ti(VI)O₆ octahedron, Ti(IV)O₄ tetrahedron, or [Ti(V)O] O₄ square pyramid). Both the height and position of the pre-edge feature A are directly related to the degree of p - d mixing,^{20,25} and therefore to the coordination geometry and oxidation state of Ti. Farges *et al.*²⁰ compiled a table of peak heights and positions of reference compounds with Ti in tetrahedral, pyramidal, and octahedral coordination. The octahedral environment of Ti in our reference BaTiO₃ is very

close to that in CaTiO₃ and rutile polymorph TiO₂; thus the absolute value of energy for feature A must also be similar. This permits direct superposition of our data with the data from Ref. 20 (Fig. 3). Excellent agreement between our data and Ti(VI) data, with respect to both the positions and heights of peak A, indicates that in all our samples, ordered and disordered alike, the majority of Ti atoms are octahedrally coordinated. According to Farges *et al.*,²⁰ it is difficult to discriminate, based on XANES measurements only, between the homogeneous system of Ti(VI) octahedral units and a heterogeneous system where a small fraction (<20%) of fivefold coordinated Ti may also be present.²⁰ However, this discrimination can be made with extended x-ray-absorption fine-structure spectroscopy (EXAFS) data.

EXAFS data and their Fourier transform magnitudes (EXAFS radial distribution functions, or ERDF's) performed in the k range between 2 and 7.5 \AA^{-1} for amorphous, quasiamorphous, and crystalline samples are shown in Fig. 4(a). Proximity of the Ba L3-edge (5247 eV) to the Ti *K*-edge limits our EXAFS analysis to a qualitative comparison of all the data sets. The spectra of the as-deposited amorphous and the quasiamorphous samples are very similar, which implies that the local environment of Ti⁴⁺ ion does not undergo detectable changes during the transformation of the amorphous (nonpolar) phase into the quasiamorphous (polar) phase [Fig. 4(b)]. As expected, these spectra do not contain higher shell EXAFS contributions [Fig. 4(a)], which are observed for the crystal-like samples, confirming that the former samples are strongly disordered. Accordingly, the ERDF's of these two groups of samples differ significantly in the region $r > 2.3$ \AA , i.e., beyond the distances corresponding to the first nearest neighbors [Fig. 4(b)]. However, ERDF's in the region $r < 2$ \AA are very similar for *all* samples [Fig. 4(b)] [note that the ERDF's in Fig. 4(b) are not corrected for the photoelectron phase shift and are therefore shifted to the left from the true interatomic distances by ≈ 0.7 \AA]. Sample to sample deviations of the amplitude, peak position, and peak width for the first nearest-neighbor peak of the ERDF are within 4%. This is possible only if the coordination number and the distributions of distances between the titanium ion and the nearest-neighboring oxygen ions are the same in all samples. Therefore both XANES and EXAFS clearly indicate that the local bonding unit of Ti in amorphous-like and crystal-like samples is octahedral and identical to that in reference BaTiO₃.

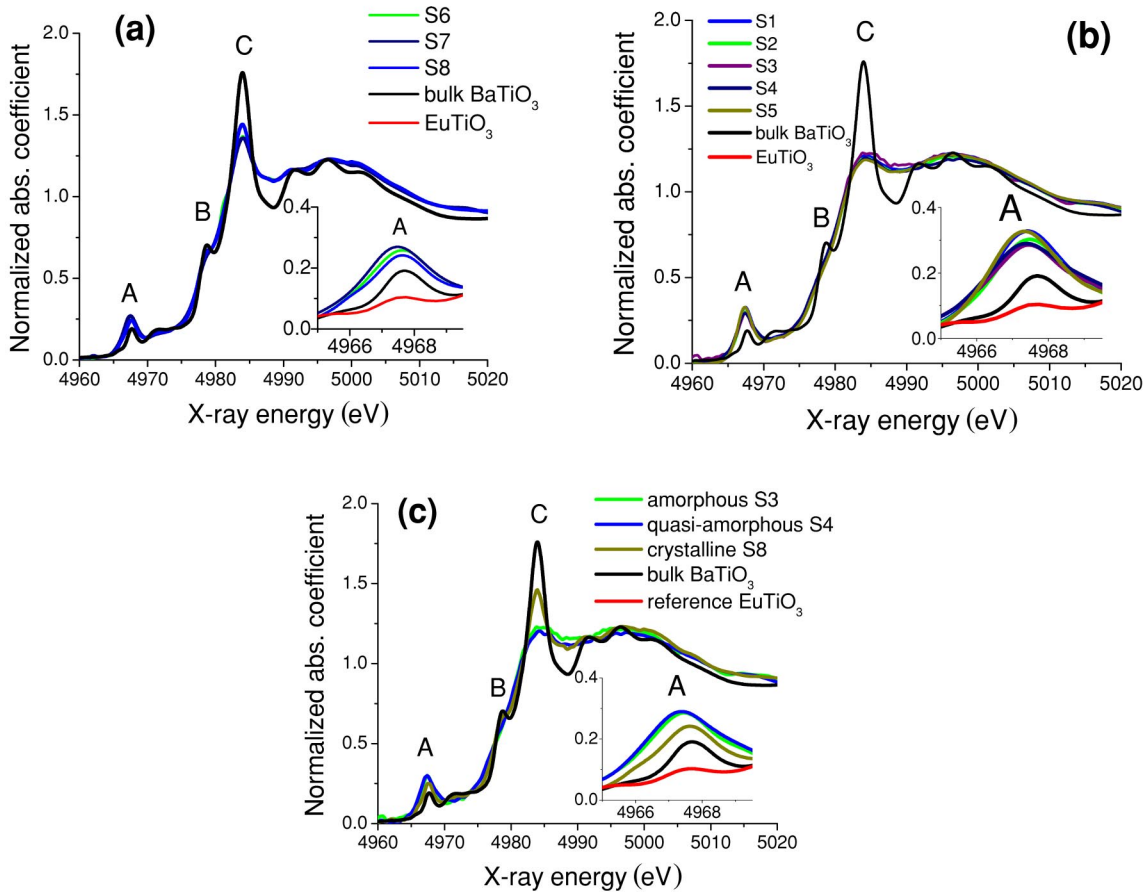


FIG. 2. (Color online) XANES spectra of crystalline-like (a) and amorphous-like (b) samples. (c) shows the superimposed spectra for the as-deposited amorphous, the quasi-amorphous, and the polycrystalline single phase films. The data for bulk BaTiO₃ and a sample of EuTiO₃ are given for comparison. Insets: the area of feature A is proportional to the square of the Ti atom off-center displacement and therefore to the strength of local dipole moment.

In this view one can interpret the intensity of feature A of XANES spectra as a measure of the displacement of the Ti ion from the center of the TiO₆ octahedron. For polycrystalline perovskites, the off-center displacement d_i (static and/or dynamic) of the Ti atom is related to the area A_i under the corresponding peak in the $1s$ - $3d$ transition region:^{28,29}

$$A_i = \frac{\gamma_i}{3} d_i^2, \quad (1)$$

where i denotes a specific perovskite system and γ_i are experimentally measured constants for various perovskites¹⁷ ($\gamma_{\text{BaTiO}_3} = 11.2 \text{ eV}/\text{\AA}^2$, $\gamma_{\text{EuTiO}_3} = 13.6 \text{ eV}/\text{\AA}^2$), and $d_{\text{EuTiO}_3} = 0.103 \text{ \AA}$ at 300 K. The strength of the local dipole moment is proportional to d_i and can be directly related to the area A_i under this XANES peak. Centrosymmetric perovskites such as EuTiO₃ also have a small peak in the energy region corresponding to the $1s$ - $3d$ transition^{17,29} due to vibrational disorder within the TiO₆ octahedra. Prior to calculating the average Ti atom displacement [Eq. (1)] in BaTiO₃ samples, the peak area for EuTiO₃ was subtracted in order to correct for thermal motion. Remarkably, the values of the Ti displacement in all samples exceeded that in bulk BaTiO₃ where $d = 0.23 \text{ \AA}$ (Table I). It is also noteworthy that the sample S8,

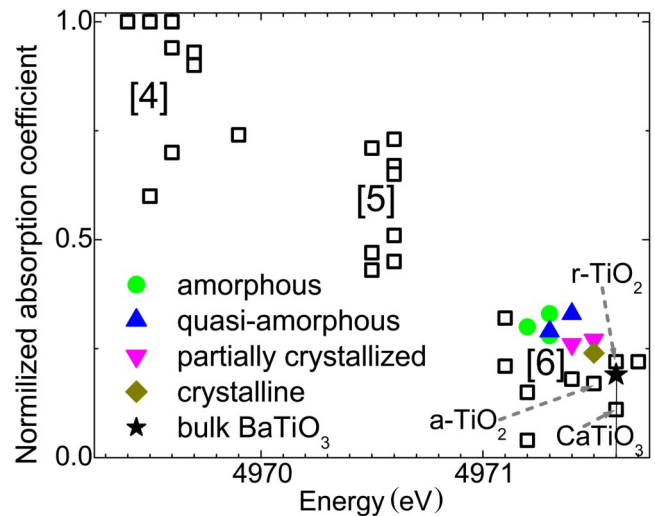


FIG. 3. (Color online) Superposition of the intensity and position of XANES feature A: (i) The domains ([4], [5], and [6]: hollow squares) for four-, five-, and sixfold coordinated Ti in different reference compounds (as in Ref. 20), aligned in absolute energy. (ii) Data for all samples and bulk BaTiO₃. The data were aligned with data reported in Ref. 20 using bulk BaTiO₃ for calibration.

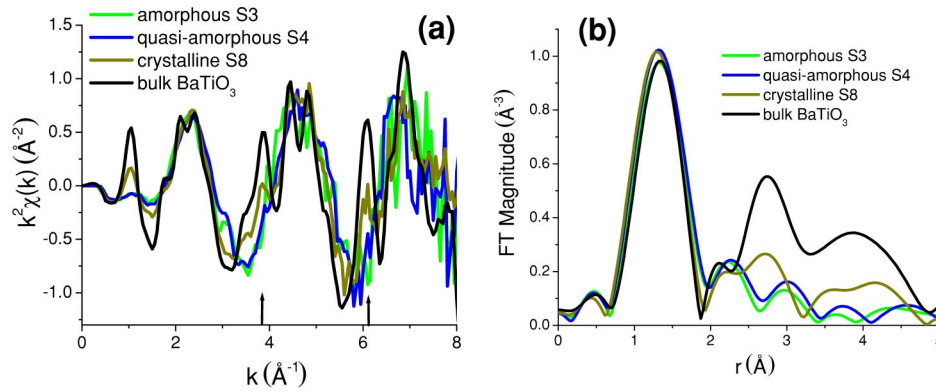


FIG. 4. (Color online) k^2 -weighted $\chi(k)$ EXAFS data (a) and the EXAFS radial distribution functions (b) of amorphous, quasiamorphous, crystalline, and bulk BaTiO_3 samples. The arrows in (a) indicate high-frequency spectral components in both crystalline BaTiO_3 samples due to the second- and higher-order nearest neighbors around Ti.

which is the most crystalline according to XRD, showed the smallest value of d , i.e., the closest to the reference BaTiO_3 . This agrees well with earlier data on other XANES features and XRD spectra of fine-crystalline BaTiO_3 .^{18,19}

One of the key results from our experimental data is that the XANES and EXAFS spectra of as-deposited amorphous and quasiamorphous samples are nearly identical with regard to their local bonding environment [Fig. 4(b)], which implies that no nucleation has taken place. This finding complements those of ED, XRD, and Ref. 1 that no detectable long-range or medium-range structural changes occur during the pulling of the films through the temperature gradient. Preservation of the local bonding unit in amorphous BaTiO_3 provides a simple explanation for the fact that according to the differential scanning calorimetry data³⁰ RF sputtered amorphous BaTiO_3 has a very low crystallization enthalpy, $-(7-9)$ kJ/mole. The titanium ion creates one of the strongest effective electric fields due to its small radius and large effective charge.¹³ This implies that most of the electrostatic binding energy in BaTiO_3 originates from Ti-O bonding. Once the TiO_6 bonding unit is assembled the enthalpy of crystallization is strongly reduced. Nearly complete preservation of the Ti local bonding unit is also observed in amorphous (glasses) and in crystalline fresnoites ($\text{Ba}_2\text{TiGe}_2\text{O}_8$ and $\text{Ba}_2\text{TiSi}_2\text{O}_8$),²¹ where Ti is tetrahedral and there is pyramidal coordination (i.e., off-centrosymmetric).

Remarkably, the dielectric constant shows only a moderate increase (from 9 to 30) during the transformation of the amorphous phase into the quasiamorphous one.¹ The latter value is significantly lower than that in crystalline BaTiO_3 , where the magnitude of the dielectric constant reaches hun-

dreds or thousands.³¹ Taking into account that the magnitude of the local dipole moment (proportional to the off-center displacement of Ti in TiO_6 octahedra) in the quasiamorphous phase is nearly twice as large as that in bulk BaTiO_3 and assuming that the dipole contribution to the pyroelectric effect is proportional to the dipole moment, our estimates show that the alignment of just 5% of the local dipoles in the quasiamorphous phase will be sufficient to produce a pyroelectric effect of the experimentally observed magnitude [5–15% of bulk BaTiO_3 (Ref. 1)]. The latter estimate was confirmed experimentally by performing polarized XANES measurements in quasiamorphous films oriented at different angles with respect to the incident synchrotron x-ray beam. The anisotropy in Ti atom displacements as measured in the plane of the film and in the perpendicular direction was found to be less than 5%.

Our results provide insight into the origin of polarity in quasiamorphous BaTiO_3 films. It is caused by (i) the existence of large off-center displacements of the Ti atoms within relatively stable TiO_6 local bonding units, and (ii) their partial alignment. In crystalline BaTiO_3 all TiO_6 octahedra are connected via the apices, and the off-center displacement of the Ti ion is a result of a long-range correlation mediated by a lattice vibration (soft phonon mode). In the absence of this interaction, Ti ions generally reside in the center of the octahedra, a tendency that is observed in a large variety of compounds containing $[\text{TiO}_6]$ local bonding units. Only a very minor fraction of these compounds is polar.^{4,32} This is in perfect agreement with a number of theoretical works^{16,33} and with the fact that BaTiO_3 grains with size below ≈ 30 nm are generally not polar^{5,6,8-10} with the exception of

TABLE I. Ti atom off-center displacements d as obtained by XANES.

| | Amorphous like | | | | | Crystal like | | | |
|-------------------------|----------------------|------|------|------------------------|------|-----------------------------------|------|-----------------------------|------|
| | Amorphous (nonpolar) | | | Quasiamorphous (polar) | | Partially crystallized (nonpolar) | | Crystalline (ferroelectric) | |
| XRD characteristics | Without peaks | | | Without peaks | | Weak diffraction peaks | | Strong diffraction peaks | |
| Sample ID | S1 | S2 | S3 | S4 | S5 | S6 | S7 | S8 | bulk |
| d , Å (± 0.01 Å) | 0.45 | 0.43 | 0.43 | 0.44 | 0.44 | 0.37 | 0.39 | 0.33 | 0.23 |

some special cases.^{11,12} This is also confirmed by the fact that the partially crystallized films are not polar, whereas the quasiamorphous films are. In the absence of long-range translational order, the origin of the off-center Ti displacement is likely to be in the asymmetry of the local octahedral environment and therefore is different from that operating in crystalline BaTiO₃. In disordered films, both amorphous (as-deposited) and quasiamorphous (pulled through the temperature gradient), such asymmetry may be caused by some neighboring octahedra being connected via edges and faces, and some via apices. Therefore the two types of films are structurally indistinguishable [Fig. 4(b)], and the magnitudes of their Ti⁴⁺ off-center displacements are the same. However, in the amorphous (nonpolar) films the displacement directions are not correlated between neighboring octahedra. In quasiamorphous (polar) BaTiO₃ films, there is a weak orientational order, which probably is generated by the gradient of mechanical strain produced in the temperature gradient and the electric field resulting from the flexoelectric effect.¹ Therefore, despite the structural similarity with the amorphous films, the quasiamorphous films are polar and can be viewed as being analogous to a poorly aligned nematic liquid

crystal, where polar molecules (rigid polar units) have a weak orientational order but lack translational order. One should note that the macroscopic polarization of the quasiamorphous films may in fact be strongly enhanced by the large in-plane compressive stress, similar to the case of stress-induced polarization in crystalline piezoelectrics. However, the influence of the strain gradient and the influence of the macroscopic stress cannot be separated here because in-plane compressive stress is a necessary condition for the existence of the quasiamorphous state. Finally, the above findings suggest that under similar conditions other noncrystalline polar phases containing stable local bonding units, for example TiO₄, TiO₆, NbO₄, NbO₆, VO₆, may also exist.

A.I.F. acknowledges support by the U.S. Department of Energy Grant No. DE-FG02-03ER15477. NSLS is supported by the Divisions of Materials and Chemical Sciences of DOE. The members of the group from the Weizmann Institute wish to acknowledge the Israel Science Foundation and US-Israel Binational Science Foundation for funding this research.

-
- ¹V. Lyahovitskaya, I. Zon, Y. Feldman, S. R. Cohen, A. K. Tagantsev, and I. Lubomirsky, *Adv. Mater. (Weinheim, Ger.)* **15**, 1826 (2003).
- ²R. Zallen, *The Physics of Amorphous Solids* (Wiley, New York, 1983).
- ³N. N. Greenwood and A. Earnshaw, *Chemistry of the Elements* (Pergamon, Oxford, 1984).
- ⁴F. Jona and G. Shirane, *Ferroelectric Crystals* (Dover, New York, 1998).
- ⁵M. T. Buscaglia, V. Buscaglia, M. Viviani, J. Petzelt, M. Savinov, L. Mitoseriu, A. Testino, P. Nanni, C. Harnagea, Z. Zhao, and M. Nygren, *Nanotechnology* **15**, 1113 (2004).
- ⁶L. Mitoseriu, C. Harnagea, P. Nanni, A. Testino, M. T. Buscaglia, V. Buscaglia, M. Viviani, Z. Zhao, and M. Nygren, *Appl. Phys. Lett.* **84**, 2418 (2004).
- ⁷Z. Zhao, V. Buscaglia, M. Viviani, M. T. Buscaglia, L. Mitoseriu, A. Testino, M. Nygren, M. Johnsson, and P. Nanni, *Phys. Rev. B* **70**, 024107 (2004).
- ⁸S. Li, J. A. Eastman, Z. Li, C. M. Foster, R. E. Newnham, and L. E. Cross, *Phys. Lett. A* **212**, 341 (1996).
- ⁹M. H. Frey and D. A. Payne, *Phys. Rev. B* **54**, 3158 (1996).
- ¹⁰M. H. Frey and D. A. Payne, *Appl. Phys. Lett.* **63**, 2753 (1993).
- ¹¹J. J. Urban, J. E. Spanier, O. Y. Lian, W. S. Yun, and H. Park, *Adv. Mater. (Weinheim, Ger.)* **15**, 423 (2003).
- ¹²C. H. Ahn, K. M. Rabe, and J. M. Triscone, *Science* **303**, 488 (2004).
- ¹³E. A. Kahn and A. J. Leyendecker, *Phys. Rev.* **135**, A1321 (1964).
- ¹⁴R. Comes, M. Lambert, and A. Guinier, *Solid State Commun.* **6**, 715 (1968).
- ¹⁵R. Comes, M. Lambert, and A. Guinier, *Acta Crystallogr., Sect. A: Cryst. Phys., Diff., Theor. Gen. Crystallogr.* **A26**, 244 (1970).
- ¹⁶I. B. Bersuker, *Phys. Lett.* **20**, 589 (1966).
- ¹⁷B. Ravel, Ph.D. thesis, University of Washington, 1995.
- ¹⁸A. I. Frenkel, M. H. Frey, and D. A. Payne, *J. Synchrotron Radiat.* **6**, 515 (1999).
- ¹⁹A. I. Frenkel, F. M. Wang, S. Kelly, R. Ingalls, D. Haskel, E. A. Stern, and Y. Yacoby, *Phys. Rev. B* **56**, 10 869 (1997).
- ²⁰F. Farges, G. E. Brown, and J. J. Rehr, *Phys. Rev. B* **56**, 1809 (1997).
- ²¹F. Farges, *J. Non-Cryst. Solids* **204**, 53 (1996).
- ²²F. Farges, G. E. Brown, and J. J. Rehr, *Geochim. Cosmochim. Acta* **60**, 3023 (1996).
- ²³F. Farges, G. E. Brown, A. Navrotsky, H. Gan, and J. J. Rehr, *Geochim. Cosmochim. Acta* **60**, 3039 (1996).
- ²⁴F. Farges, G. E. Brown, A. Navrotsky, H. Gan, and J. J. Rehr, *Geochim. Cosmochim. Acta* **60**, 3055 (1996).
- ²⁵Z. Y. Wu, G. Ouvrard, P. Gressier, and C. R. Natoli, *Phys. Rev. B* **55**, 10 382 (1997).
- ²⁶E. A. Stern and S. M. Heald, in *Handbook on Synchrotron Radiation*, edited by E. E. Koch (North-Holland, New York, 1983), Vol. 1, Chap. 10.
- ²⁷L. A. Grunes, *Phys. Rev. B* **27**, 2111 (1983).
- ²⁸B. Ravel, E. A. Stern, R. I. Vedrinskii, and V. Kraizman, *Ferroelectrics* **206**, 407 (1998).
- ²⁹V. L. Kraizman, A. A. Novakovich, R. V. Vedrinskii, and V. A. Timoshevskii, *Physica B* **209**, 35 (1995).
- ³⁰J. P. Chu, S. F. Wang, S. J. Lee, and C. W. Chang, *J. Appl. Phys.* **88**, 6086 (2000).
- ³¹I. Bunget and M. Popescu, *Physics of Solid Dielectrics* (Elsevier, Amsterdam, 1984).
- ³²R. W. G. Wyckoff, *Crystal Structures* (Interscience, New York, 1967).
- ³³D. Vanderbilt, *Curr. Opin. Solid State Mater. Sci.* **2**, 701 (1997).